Aerosol and Air Quality Research, 18: 2764–2774, 2018

ISSN: 1680-8584 print / 2071-1409 online
doi: 10.4209/aaqr.2017.11.0450

Characteristics of Organic Carbon and Elemental Carbon in Atmospheric Aerosols in the Urban Area in Beibei, a Suburb of Chongqing

Xiaole Peng[1], Qingju Hao[1], Tianxue Wen[2], Dongsheng Ji[2], Zirui Liu[2], Yuesi Wang[2], Xinhua He[1], Xiaoxi Li[1], Changsheng Jiang[1*]

[1] *Key Laboratory of Eco-environments in Three Gorges Reservoir Region (Ministry of Education), College of Resources and Environment, Southwest University, Chongqing 400715, China*
[2] *State Key Laboratory of Atmospheric Boundary Layer Physics and Atmospheric Chemistry, Institute of Atmospheric Physics, Chinese Academy of Sciences, Beijing 100029, China*

ABSTRACT

To investigate the pollutive characteristics of atmospheric carbonaceous aerosols in Beibei District, a suburb of Chongqing Municipal City, graded aerosol samples were continuously collected by cascade impactors over one year, from March 2014 to February 2015. Carbonaceous aerosols, including organic carbon (OC) and elemental carbon (EC), were detected by a DRI 2001A carbon analyzer. The results showed that the average annual concentrations of OC and EC in the $PM_{2.1}$ were 16.3 ± 7.6 and 1.8 ± 0.7 μg m^{-3}, and in the $PM_{9.0}$ were 25.0 ± 9.6 and 3.2 ± 1.2 μg m^{-3}, respectively. On the one hand, a more seasonal distribution of OC concentrations appeared in the $PM_{2.1}$ (winter > spring > summer > autumn) than in the $PM_{9.0}$ (winter ≈ spring ≈ summer > autumn); furthermore, whereas the OC significantly positively correlated with wind speed for both the $PM_{2.1}$ ($P < 0.05$) and the $PM_{9.0}$ ($P < 0.01$), it was negatively correlated with relative humidity ($P < 0.05$) for the latter. On the other hand, both the $PM_{2.1}$ and the $PM_{9.0}$ exhibited a more seasonal distribution of EC concentrations (winter > spring > summer > autumn), and the EC in the $PM_{2.1}$ significantly negatively correlated with temperature ($P < 0.05$). Additionally, both the OC and the EC were concentrated mainly in the fine particles (< 2.10 μm), and the size distributions of the OC in all four seasons displayed a bi-modal pattern that peaked in the size ranges of 0.43–0.65 μm (for fine particles) and 4.7–5.8 μm (for coarse particles), whereas the EC displayed a uni-modal pattern that peaked in the size range of 4.7–5.8 μm (for coarse particles). Furthermore, the correlations between the OC and the EC were analyzed, and the SOC (secondary organic carbon) in the $PM_{2.1}$ was estimated using the primary OC/EC ratio. It was found that the OC highly significantly correlated with the EC ($P < 0.01$), with the average annual concentration of the SOC being 6.3 ± 5.9 μg m^{-3}, which accounted for 33.5 ± 22.6% of the OC. Analyzing the sources of the pollutive atmospheric aerosol in Beibei further demonstrated that it mainly originated in biomass burning, gasoline-vehicle exhaust, and coal combustion.

Keywords: Organic carbon; Elemental carbon; Size distribution; Seasonal patterns; Atmospheric aerosol.

INTRODUCTION

Carbonaceous aerosols, as an important component of atmospheric aerosols, are typically classified as EC (elemental carbon) and OC (organic carbon). EC, also known as black carbon or soot, including pure carbon and graphite carbon, originates mainly from coal combustion, vehicle emission and wood burning (Liu *et al.*, 2015). In contrast, OC can be directly emitted from sources such as POC (primary organic carbon) and SOC (secondary organic carbon), which are formed from the products of atmospheric chemical reactions through low vapor pressure, proper temperature and sunlight in the atmosphere. Atmospheric aerosols not only have important effects on the extinction of solar radiation, but also affect atmospheric long-wave radiation. In general, EC is a strongly absorbing aerosol, which has significant influence on visibility, accounting for about 20% of the visibility reduction compared with other aerosol particles (Deng *et al.*, 2008), while OC can scatter solar radiation (Kirkevag *et al.*, 2013). As a result, both of them can reduce atmospheric visibility and affect the global climate change by changing the radiation characteristics of cloud and precipitation process (Jacobson *et al.*, 2001). Moreover, EC and OC can also enter human's lungs through respiration and cause chronic respiratory diseases, even trigger lung cancer (Yang *et al.*, 2003; Pope *et al.*, 2006; Mauderly *et al.*, 2008).

* Corresponding author.
E-mail address: jiangcs@126.com

In recent years, the analysis of the pollution characteristics of carbonaceous aerosols in atmosphere has become a hot topic around the world (Kumar and Yadav, 2016; Chen *et al.*, 2017a). The distributions of carbon fractions in indoor and outdoor total carbon (TC, OC + EC) pointed to the contributions of motor vehicle exhaust and coal-combustion, and about 90% of carbonaceous particles in indoor air resulted from penetration of outdoor pollutants, while indoor sources contributed only 10% of the indoor carbonaceous particles (Cao *et al.*, 2012). At eight sites in four Chinese cities (Hong Kong, Guangzhou, Shenzhen and Zhuhai) of the Pearl River Delta Region, the OC and EC in $PM_{2.5}$ and $PM_{9.0}$ were strongly correlated (Cao *et al.*, 2003). The distributions of eight carbon fractions (OC_1, OC_2, OC_3, OC_4, EC_1, EC_2, EC_3 and OPC [optically detected pyrolyzed carbon]) indicated that the biomass burning, coal combustion and motor-vehicle exhaust were all contributed to these carbonaceous aerosols in Tianjin, China (Gu *et al.*, 2010).

Chongqing, known as a "fog city" for the serious air pollution, is an important industrial mega-city in southwest China. At present, a number of studies on the carbonaceous aerosol pollution in the atmosphere of Chongqing had been reported. For example, the seasonal characteristics of OC and EC in $PM_{2.5}$ were in the order of winter > fall > spring > summer in the hinterland of Wanzhou, Chongqing, located in the Three Gorges Reservoir region along the Yangtze River (Zhang *et al.*, 2015). The OC and EC concentrations in PM_{10} were significantly correlated to each other both in spring and in autumn, Chongqing, implying the existence of similar emission sources such as coal combustion, and the SOC was presented as the OC/EC ratios generally exceeded 2.0 (Ye *et al.*, 2007). However, the pollution sources of carbonaceous aerosols were little reported in those studies. Moreover, the particle size distribution was also rarely reported. Therefore, in this study, carbonaceous aerosol samples were collected by the Anderson sampler inertial impactor over a one-year period from March 2014 to February 2015, and the data measured from these samples were analyzed to reveal the characteristics of seasonal changes in OC and EC and their particle size distribution. In addition, the main pollution sources of OC and EC in the Beibei Suburb were determined by the correlation and principal component analysis, in order to provide a rational basis for the control and management of the aerosol pollution caused by OC and EC.

METHOD AND MATERICALS

Site Location and Sampling Method

The sampling site (29°48′43″N, 106°24′58″E) locates at the rooftop (282 m a.s.l.) of the College of Resources and Environment building (35 m above ground) at the Southwest University campus in the Beibei suburb, Chongqing Municipal City, China (Fig. 1). The Beibei suburb is surrounded by the Zhongliang Mountain (1,000 m a.s.l. in the peak) in the south and the Jinyun Mountain (951 m a.s.l. in the peak) in the north. The local air circulation in the sampling site is little affected by nearby educational and residential buildings with some small ups and downs. The site, representing a typical urban environment in the Beibei suburb of the Chongqing City, is about 30 m to a main city traffic road and about 800 m to the south of the highway intersection and has no direct industrial pollution sources within a 5-km distance.

The aerosol particles grouped as < 0.43, 0.43–0.65, 0.65–1.1, 1.1–2.1, 2.1–3.3, 3.3–4.7, 4.7–5.8, 5.8–9.0 and 9.0–100 μm in size were collected by an Andersen Impact Grading Sampler (Andersen, Series20-800, USA), respectively. The sampling flow rate was 28.30 L min^{-1}, and the sampling filters were the polyester fiber films (Thermoelectric, USA). A 48-hour continuous air sampling was taken every two weeks from March 2014 to February

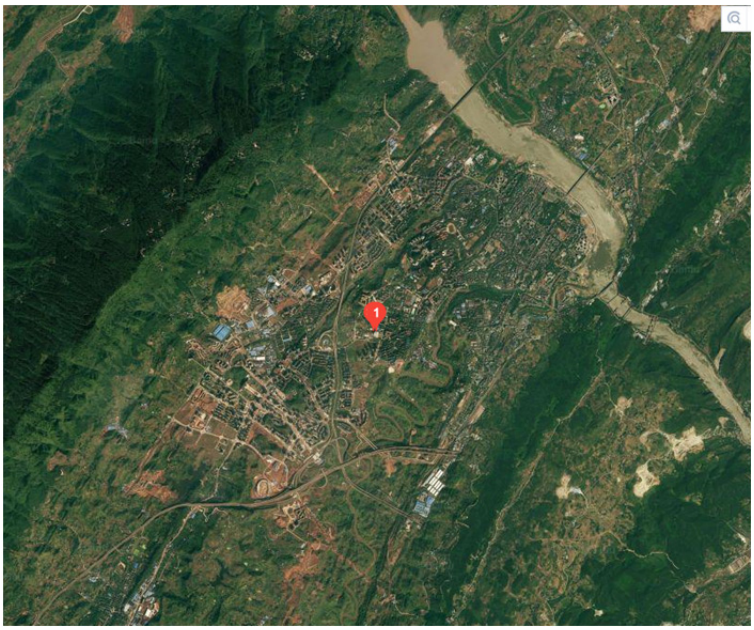

Fig. 1. A sky view of sampling site in the urban area of Beibei (29°48′43″N, 106°24′58″E), Chongqing, Southwest China.

2015 (from 11 a.m. on first day to 11 a.m. on third day). During the experiment, a total of 171 filters from 19 valid samplings were obtained and stored in refrigerators at 4°C for further analyses.

Carbonaceous Aerosol Analysis

The samples were analyzed for OC and EC using DRI Model 2001 Thermal/Optical Carbon Analyzer. And the IMPROVE thermal/optical reflectance (TOR) protocol (Chow *et al.*, 1993, 2001, 2004b) was used for the carbon analysis. In a non-oxidizing helium (He) atmosphere, a 0.5025 cm^2 punch aliquot of a sample film was stepwise heated from 140°C (OC_1), 280°C (OC_2), 480°C (OC_3), through 580°C (OC_4). The ramp-up to the next temperature or atmosphere began when the flame ionization detector (FID) response returned to a baseline or a constant value under the condition that the time spent in any segment (OC_1, OC_2, etc.). When this condition had been reached in the OC_4 segment, the 2% O_2/98% He was introduced and peaks were integrated at 580°C (EC_1), 740°C (EC_2), and 840°C (EC_3), respectively. The carbon that evaporated at each temperature was catalyzed into carbon dioxide (CO_2) by manganese dioxide, then reduced to methane (CH_4) for quantification with a flame ionization detector. As the temperature increased in the inert helium, some of the organic carbon was pyrolyzed into black carbon, which made the carbon and EC peaks difficult to be distinguished. Therefore, the 633-nm He-Ne laser was used to monitor the light intensity of the filter film during the measurements. The changes in the light intensity clearly indicated the starting point of oxidation to EC. To ensure a distinction between OC and EC, the seven fractions (OC_1, OC_2, OC_3, OC_4, EC_1, EC_2 and EC_3) were separately reported in the data sheet. In addition, the IMPROVE protocol defined OC as $OC_1 + OC_2 + OC_3 + OC_4$ and EC as $EC_1 + EC_2 + EC_3$, respectively.

Quality Assurance and Quality Control (QA/QC)

All samples were collected on polyester fiber filters (81 mm in diameter) during the study period. The polyester fiber filters were pre-fired (2 h at 800°C) to remove all organic materials and weighed before and after sampling using a micro-balance with a sensitivity of ± 0.01 mg. The filters were conditioned in a dryer at 25 ± 3°C under a relative humidity of 22 ± 3% for 72 h before each weighing. After reweighing, the sampling filters were immediately stored in a freezer at –20°C to avoid the loss of semi-volatiles. The samplers were cleaned using an ultrasonic bath before sampling. In addition, the sampling flow rates were calibrated before each sampling and monitored using a flow meter during each sampling.

Moreover, the analyzer was calibrated with known quantities of CH_4 every day. Replicate analyses were performed at the rate of one per group of ten samples. Sixteen blank filters were also analyzed, and the sample results were corrected by the average of the blank concentrations. The difference determined from the replicate analyses was less than 5% for the total carbon (TC, OC + EC) and 10% each for OC and EC (Cao *et al.*, 2003).

Statistic Analyses

The figures were plotted by the Origin 9.1 software. Statistical analyses (correlation and principal component analyses) were performed with a SPSS 17.0. Correlation between meteorological factors and OC or EC as well as the OC and EC in $PM_{2.1}$ were made by the Pearson correlation coefficients to infer the influence of meteorological factors on OC, EC and the origin of carbonaceous aerosols in atmosphere. Moreover, the principal component analysis (PCA) was used to classify and analyze the seven carbonaceous aerosols of OC_1, OC_2, OC_3, OC_4, EC_1, EC_2 and EC_3 in the $PM_{2.1}$ to explore the main sources of carbonaceous aerosol in the Beibei suburb.

RESULTS

Temporal OC and EC

The particulate matters (PM) collected by an Andersen sampler were divided into nine size groups of < 0.43, 0.43–0.65, 0.65–1.1, 1.1–2.1, 2.1–3.3, 3.3–4.7, 4.7–5.8, 5.8–9.0 and 9.0–100 μm. In order to analyze the characteristic of the particulate matter easily, the particulate matter collected was divided into two sizes as the $PM_{2.1}$ (< 2.10 μm) and $PM_{9.0}$ (< 9.00 μm).

Over the whole observation period, the average concentration of TC (total carbon, OC + EC) in $PM_{2.1}$ was 18.1 ± 8.0 μg m^{-3}, and the average concentration of OC was 16.3 ± 7.6 μg m^{-3}, which accounted for 89.3 ± 3.2% of the TC, while, the average concentration of EC was 1.8 ± 0.7 μg m^{-3}. As for the $PM_{9.0}$, the average concentration of TC in $PM_{9.0}$ was 28.2 ± 10.3 μg m^{-3}, and the average concentration of OC was 25.0 ± 9.7 μg m^{-3}, which accounted for 88.1 ± 4.1% of the TC. On the other hand, the average concentration of EC was 3.2 ± 1.3 μg m^{-3} (Table 1).

Table 1. Concentrations of elemental carbon (EC), organic carbon (OC), and TC (total carbon (TC, OC + EC)) in $PM_{2.1}$ and $PM_{9.0}$ in the Beibei suburb of Chongqing Municipal City, Southwest China.

Season	$PM_{2.1}$ (μg m^{-3})			$PM_{9.0}$ (μg m^{-3})		
	EC	OC	TC	EC	OC	TC
Spring	2.1 ± 0.4	18.8 ± 8.05	20.9 ± 8.0	3.9 ± 1.2	28.2 ± 9.9	32.0 ± 9.8
Summer	1.6 ± 0.6	16.0 ± 3.2	17.6 ± 3.2	3.0 ± 1.0	29.4 ± 6.0	32.4 ± 6.2
Autumn	1.4 ± 0.4	10.5 ± 2.4	11.8 ± 2.6	2.2 ± 1.0	15.8 ± 2.3	17.9 ± 2.7
Winter	2.3 ± 1.0	20.7 ± 12.0	23.1 ± 12.9	4.0 ± 1.3	27.0 ± 13.3	31.0 ± 14.4
Average	1.8 ± 0.7	16.3 ± 7.6	18.1 ± 8.0	3.2 ± 1.3	25.0 ± 9.7	28.2 ± 10.3

Data are means ± SD (spring: $n = 5$; summer: $n = 5$; autumn: $n = 5$; winter: $n = 4$).

The concentration of OC in $PM_{2.1}$ in Beibei showed the following seasonal distribution as winter (20.7 ± 12.0 μg m^{-3}) > spring (18.8 ± 8.05 μg m^{-3}) > summer (16.0 ± 3.2 μg m^{-3}) > autumn (10.5 ± 2.4 μg m^{-3}). In contrast the concentration of OC in $PM_{9.0}$ showed the seasonal distribution as summer (29.4 ± 6.0 μg m^{-3}) ≈ spring (28.2 ± 9.9 μg m^{-3}) ≈ winter (27.0 ± 13.3 μg m^{-3}) > autumn (15.8 ± 2.3 μg m^{-3}). And the concentrations of EC in both the $PM_{2.1}$ and $PM_{9.0}$ at Beibei presented a seasonal distribution of winter > spring > summer > autumn.

OC and EC as a Function of Particulate Size

The size of particle was the most basic physical characteristic of atmospheric particulates, which can determine the residence time, transmission distance and mechanism of particle removal in the atmosphere (Spracklen *et al.*, 2009). So, the characteristics of OC and EC size distribution were important to the study on the formation and transformation of atmospheric aerosols, the characteristics of dry and wet deposition, and the global effects of aerosols (Mcmurry *et al.*, 1989).

During the observation period, about 61.5% of OC and 50% of EC were concentrated in fine particles (Fig. 2). And OC has the highest concentration in the size of 0.43–0.65 μm (4.8 ± 2.2 μg m^{-3}) and 0.65–0.1 μm (4.9 ± 2.7 μg m^{-3}), which accounted for 18.0% and 18.4% of the TOC (the total of OC in all particle sizes) concentration, respectively. There was the highest concentration of EC in the size of < 0.43 μm (0.7 ± 0.4 μg m^{-3}), which accounted for 20.1% of TEC (the total of EC in all particle sizes) concentration.

In order to illustrate the particle size distribution of carbonaceous aerosol in Beibei suburb, logarithmic model was taken to analyze the particle size distribution of OC and EC, and using the concept of differentiation, defined as:

$$dM = M(lgD_p) \times dlgD_p \quad (1)$$

In the formula, dM represents the mass concentration of particles in the range of lgD_p to $lgD_p + dlgD_p$; $M(lgD_p)$ represents the distribution function of mass concentration; D_p is the average value between the particle size segments, then taking $dM/dlgD_P$ as the horizontal axis and D_P as the vertical axis to obtain the OC and EC distribution in different size particles.

The size distributions of OC in four seasons all showed a "bi-modal" according to the Fig. 3, with peaks in the range size of 0.43–0.65 μm in fine particle, and 4.7–5.8 μm in coarse particle. While EC was more complicated, EC showed a "uni-modal" with peak in the range size of 4.7–5.8 μm in coarse particle, and in fine particle, EC was messy, with no obvious peak characteristics in four seasons.

Estimation of Secondary Organic Carbon

It has been recognized for decades that SOC related to haze, visibility, climate and heath (Griffin *et al.*, 2002). The ratio of OC/EC was used to identify the emissions and transformation characteristics of carbon particles, and SOC existed when the ratio exceeded 2.0 (Turpin *et al.*, 1995; Chow *et al.*, 1996). Moreover, the larger the ratio of OC/EC was, the more serious the SOC pollution was, and this approach had been adopted by numerous studies (Gu *et al.*, 2010; Li *et al.*, 2015).

During the whole observation period, the average ratio of OC/EC (9.3 ± 3.7) was greater than 2.0, and the highest OC/EC ratio (11.4 ± 5.4) appeared in summer while the lowest (8.0 ± 2.2) in autumn (Table 2), indicating the existence of SOC in four seasons.

Although there was no simple direct analytical technique available, only several indirect methodologies have been applied in the evaluation of SOC formation in ambient aerosols (Turpin and Huntzicker, 1991; Pandis *et al.*, 1992; Turpin and Huntzicker, 1995). According to Turpin *et al.* (1990), the production of SOC in $PM_{2.1}$ can be calculated from the following equation:

$$SOC = OC_{tot} - EC \times (OC/EC)_{pri} \quad (2)$$

where OC_{tot} was the OC in $PM_{2.1}$, $(OC/EC)_{pri}$ was the ratio

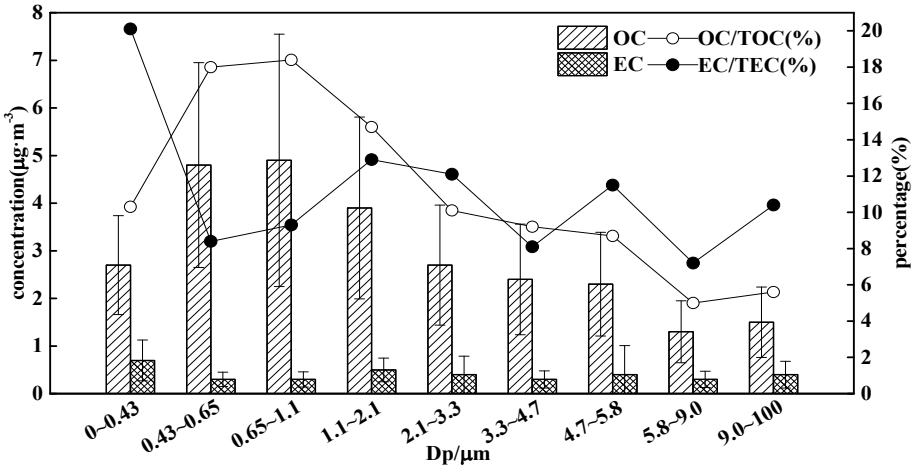

Fig. 2. Averaged concentrations of organic carbon (OC) and elemental carbon (EC) in each particle size, and percentages of OC and EC in each particle size to TOC (the total OC in all particle sizes) and TEC (the total EC in all particle sizes) in Beibei District, a suburb of Chongqing Municipal City, Southwest China.

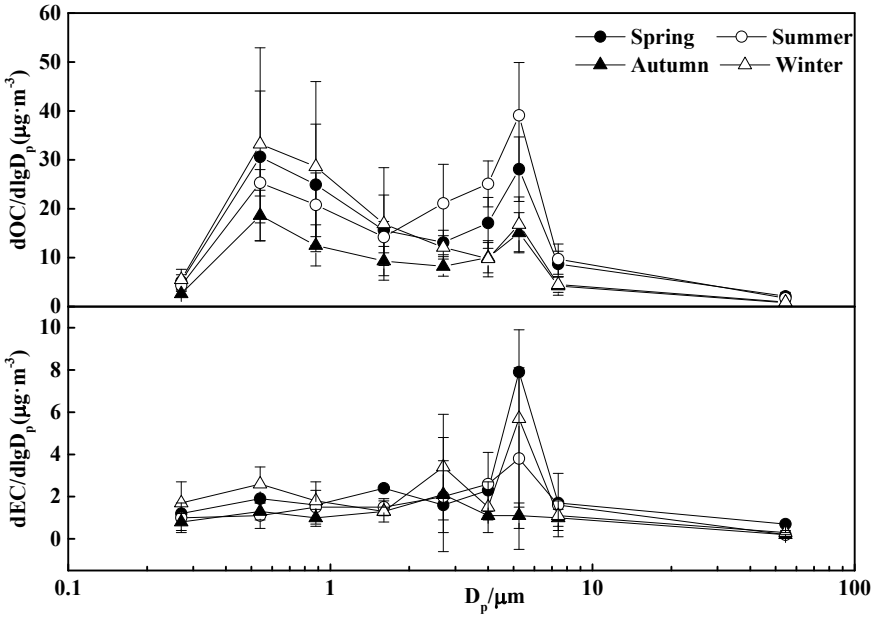

Fig. 3. Size distribution of OC and EC in four seasons.

Table 2. Concentrations of secondary organic carbon (SOC), ratios of SOC/organic carbon (OC) and OC/EC (elemental carbon) in $PM_{2.1}$ during four seasons in 2014 in the Beibei suburb of Chongqing Municipal City, Southwest China.

Season	SOC (μg m^{-3})	SOC/OC (%)	OC/EC
Spring	7.0 ± 8.5	28.6 ± 33.2	9.0 ± 4.0
Summer	7.4 ± 4.5	44.5 ± 20.6	11.4 ± 5.4
Autumn	3.1 ± 2.3	27.8 ± 17.5	8.0 ± 2.2
Winter	7.9 ± 7.2	32.9 ± 18.2	8.6 ± 2.0
Annual	6.3 ± 5.9	33.5 ± 22.6	9.3 ± 3.7

Data are means ± SD (spring: n = 5; summer: n = 5; autumn: n = 5; winter: n = 4).

of OC and EC in $PM_{2.1}$, produced during the primary emission process. However, the value of $(OC/EC)_{pri}$ related to the emission of each pollution source, which was not easily to be calculated. Turpin and Huntzicker (1991) found that the lowest ratio of OC/EC could approximately equal to $(OC/EC)_{pri}$ in a certain period. Thus, Eq. (2) can be rewritten as:

$$SOC = OC_{tot} - EC \times (OC/EC)_{min} \quad (3)$$

The ratio of OC/EC was affected by meteorology of the region, diurnal and seasonal fluctuations in emissions and aerosol transportation (Ali *et al.*, 2016), the average of the three minimum OC/EC ratios (5.48) in $PM_{2.1}$ during the whole sampling time was selected to replace $(OC/EC)_{pri}$, and was substituted into Eq. (3) to estimate the concentration of SOC in each sample, then calculate the average concentration of SOC for the whole year and each season.

The calculated average concentrations of SOC in $PM_{2.1}$ over the whole year was 6.3 ± 5.9 μg m^{-3}, accounting for 33.5 ± 22.6% of the OC in $PM_{2.1}$ (Table 2). Greater SOC distributions over the four seasons patterned as winter (7.9 ± 7.2 μg m^{-3}) > summer (7.4 ± 4.5 μg m^{-3}) ≈ spring (7.0 ± 8.5 μg m^{-3}) > autumn (3.1 ± 2.3 μg m^{-3}). In addition, greater seasonal distribution of SOC/OC ratios ranked as summer (44.5 ± 20.6%) > winter (32.9 ± 18.2%) > spring (28.6 ± 33.2%) ≈ autumn (27.8 ± 17.5%).

DISCUSSIONS

Temporal OC and EC

The concentrations of OC in both $PM_{2.1}$ and $PM_{9.0}$ in Beibei were accounted for ~90% of the TC, making it the predominant carbon contributor (Table 1). Also in Beibei, the annual average concentrations of OC and EC in $PM_{2.1}$ or $PM_{9.0}$ in this study were 16.3 ± 7.6 and 1.8 ± 0.7 μg m^{-3} or 25.0 ± 9.7 and 3.2 ± 1.3 μg m^{-3}, respectively (Table 1), while OC and EC in a similar size of PM_{10} ten years ago were 54.1 ± 15.6 and 6.2 ± 2.0 μg m^{-3} (Ye *et al.*, 2006). Similarly, the concentrations of OC and EC in $PM_{2.5}$ were 23.6 and 8.7 μg m^{-3} in 2013 in Wanzhou suburb of Chongqing (Zhang *et al.*, 2015), which might be due to more industrial pollution emissions from the construction of Wanzhou economic and technological development area, where is about 220 km away of east from Beibei. Meanwhile, the average concentrations of OC and EC in $PM_{2.5}$ were 19.0 ± 13.3 and 4.6 ± 2.6 μg m^{-3} between May 2012 and April 2013 in Chengdu, where is about 250 km away of west from Beibei (Chen *et al.*, 2014). These results indicated that the air pollution in Beibei had been obviously alleviated in recent years, though the sizes of

those referred aerosols were different with present study ($PM_{2.1}$ and $PM_{9.0}$) and previous studies from Beibei (PM_{10}), Wanzhou ($PM_{2.5}$) and Chendu ($PM_{2.5}$).

The concentrations of OC and EC presented different seasonal characteristics because of the variations in climate and pollution sources (Lang *et al.*, 2017). During one year observation period, greater OC concentration in $PM_{2.1}$ over the four seasons ranked as winter (20.7 ± 12.0 μg m^{-3}) > spring (18.8 ± 8.05 μg m^{-3}) > summer (16.0 ± 3.2 μg m^{-3}) > autumn (10.5 ± 2.4 μg m^{-3}). While Chen *et al.* (2017b) found that the traditional activity of preserving meat with smoking in southwestern China was a major source of particulate pollution in winter. Therefore, the higher concentration of OC in winter might be due to more biomass being burned to produce smoking for meat preservation, the lower temperature and higher atmospheric stability, which could lead to the difficult proliferation of pollutants, while the more motor-vehicle exhaust under low temperature in winter was probably another reason. For $PM_{9.0}$, the concentration of OC showed the seasonal distribution as summer (29.4 ± 6.0 μg m^{-3}) ≈ spring (28.2 ± 9.9 μg m^{-3}) ≈ winter (27.0 ± 13.3 μg m^{-3}) > autumn (15.8 ± 2.3 μg m^{-3}) (Table 1). More rainfall was probably one of the reasons why the concentration of OC in autumn (62.1 mm) was lowest among the four seasons (18.2, 27.6 and 2.9 mm in spring, summer and winter). Compared with the OC concentration in $PM_{2.1}$, the OC concentration in $PM_{9.0}$ in spring and summer was rapidly increased, probably due to the increase of coarse-grained biomass aerosol in spring and summer, like pollen (Pavuluri *et al.*, 2013). Whether in $PM_{2.1}$ or $PM_{9.0}$, the concentration of EC was the highest in winter, which may be caused by the lower temperature and higher atmospheric stability in winter, and lowest in autumn, which may be caused by more rainfall in autumn.

During one-year observation period, the different seasonal characteristic of OC and EC may be related to the meteorological factors, such as precipitation (PRE), temperature (TEM), relative humidity (RHU), sunshine radiation (SSD) and wind speed (Win). In $PM_{2.1}$ and $PM_{9.0}$, the relationships of the concentration of OC, EC or TC with PRE, TEM, RHU, SSD and Win had been estimated through correlation analysis (Table 3). The table revealed that OC and TC have a significant positive relationship with Win ($P < 0.05$) in $PM_{2.1}$, and their relationship in $PM_{9.0}$ with Win were fairly good ($P < 0.01$), though the relationships were statistically significant, the range of wind speed was quite small (0.9–1.7 m s^{-1}) during the entire sampling period. Thus the wind speed does influence the concentration of OC and TC at Beibei but not strongly. EC is negatively correlated with TEM ($P < 0.05$) in $PM_{2.1}$, meaning that as the air temperature decreases, the concentration of EC will increase instead, which reflects the highest concentration of EC appeared in winter. There were no significant correlations between EC and five meteorological factors in $PM_{9.0}$.

OC and EC as a Function of Particulate Size

Whitby *et al.* (1972) first described the basic size distribution of atmospheric particles by Minnesota Aerosol Analyzing System. The size distributions of atmospheric particles were described as three parts: (1) Aitken (< 0.1 μm), (2) accumulation mode (0.1–2 μm), and (3) coarse mode (> 2 μm). Then John *et al.* (1990) found that there were two sub-modes (the condensation and droplet mode) in the accumulation mode, the mode with the peak at 0.2 μm was "condensation mode," which might mainly be produced by the gas-phase reaction. A mode with the peak at 0.7 μm was the "droplet mode," which might be mainly produced by the fine particle nucleation reaction in droplets (John *et al.*, 1990).

The particles in the accumulation mode can stay a long time in the air, and not easy to be degraded. At the same time, the size of particles in the accumulation mode was similar to the wavelength of solar shortwave radiation, indicating that the particles have a high light extinction, and an important impact on global climate and human health (Yu *et al.*, 2010). During the whole observation period, about 61.5% of OC and 50% of EC were concentrated in the fine particles (< 2.10 μm) (Fig. 2), while, the particles with the size of 0.1–2 μm were in accumulation mode, indicating that most of OC and EC were mainly concentrated in accumulation mode, which can greatly influence the global climate and human health.

The particle size of OC showed a "bi-modal" distribution in all four seasons (Fig. 3). The fine particle in the size of 0.43–0.65 μm was in Aitken mode, which may be caused by the vehicle exhausts (Yu *et al.*, 2009) and biomass combustion (Glaser *et al.*, 2005), and the coarse particle in 4.7–5.8 μm was in coarse mode, which may be caused by the dust, soil suspended matter (Bi *et al.*, 2005) and biological aerosols, such as microorganisms, plant fragments, pollen, etc. (Lan *et al.*, 2011). While EC in four seasons only shows a coarse peak in the size of 4.7–5.8 μm, which may be caused by the direct combustion emissions of the EC

Table 3. Correlation analyses between meteorological factors and organic carbon (OC), elemental carbon (EC) or total carbon (TC) in the $PM_{2.1}$ and $PM_{9.0}$ in Beibei suburb of Chongqing Municipal City, Southwest China.

Meteorological factors	$PM_{2.1}$			$PM_{9.0}$		
	EC	OC	TC	EC	OC	TC
PRE (mm)	–0.01	–0.24	–0.23	–0.03	–0.22	–0.21
TEM (°C)	–0.48*	–0.16	–0.19	–0.42	–0.17	–0.12
RHU (%)	0.22	–0.29	–0.25	0.24	–0.51*	–0.45
SSD (h)	–0.31	0.08	0.05	–0.21	0.37	0.33
Win (m s^{-1})	0.15	0.55*	0.53*	0.04	0.62**	0.58**

* and ** represent significant correlations at $P < 0.05$ and $P < 0.01$.

mixed with the surface dust generated by tire brake wear, road dust, industrial emissions and construction activities (Salma *et al.*, 2002).

Estimation of Secondary Organic Carbon

The annual average concentration of SOC was 6.3 ± 5.9 μg m^{-3}, which accounted for 33.5 ± 22.6% of OC, indicating that SOC was an important component of carbonaceous aerosols (Table 2). Such results were lower than those (SOC: 9.0 ± 10.5 μg m^{-3}; SOC/OC: 32.3 ± 7.9%) in Wanzhou (Zhang *et al.*, 2015), reflecting that the pollution of SOC in Beibei was less serious than that in Wanzhou.

Previous research results show that the formation of SOC is from VOCs via two processes: condensable organic compounds through oxidation reaction and the nucleation and condensation of vapors (Pandis *et al.*, 1992). The photochemical activity and atmospheric temperature therefore play important roles in the SOC formation. An investigation into the effects of atmospheric temperature on SOC formation showed that SOC in $PM_{2.5}$ had a significant negative correlation with temperature (R^2 = 0.42) (Niu *et al.*, 2012). Lower temperatures were favorable for absorption and condensation of semi-volatile organic compounds on existing particles (Pandis *et al.*, 1992; Odum *et al.*, 1996). However, the mechanism of SOC formation during wintertime is still arguable. For example, the photochemical reaction resulting in SOC formation was significant in winter (Huang *et al.*, 2014). The water-soluble organic products through a gas-phase photochemistry dissolving into the aqueous phase could react further to form low volatility products that were largely partitioned in the particle phase (Lim *et al.*, 2010), but gaseous oxidant concentrations decreased significantly, suggesting a reduced production of secondary aerosols through gas-phase reactions in winter (Zheng *et al.*, 2015). Thus it might be reasonable to infer that high average SOC concentrations (7.9 ± 7.2 μg m^{-3}) in winter was estimated as a result of lower temperature and high VOCs emissions in this study. However, it is difficult to conclude which is the dominant pathway for the chemical processes (OH chemistry, aqueous-phase chemistry or NO_3 chemistry). Compared with results in winter, there was an overall trend towards lower SOC concentration (7.4 ± 4.5 μg m^{-3}) but a higher percentage of SOC in the OC (44.5 ± 20.6%) in summer, which might be caused by the more intense solar radiation during the summer and it will provide favorable conditions for photochemical activity and SOC production.

Sources of Carbonaceous Aerosols

The ratio of OC/EC can be used not only to evaluate the existence of SOC, but also to analyze the main pollution sources and the emission characteristics of carbonaceous aerosols (Gu *et al.*, 2010). When the ratios of OC/EC ranged 1.0–4.2, 2.5–10.5 and 32.9–81.6, which indicated that the pollution sources were vehicle exhaust emission, coal emission and cooking emission, respectively (Schauer *et al.*, 1999a, b, 2001, 2002a, b; He *et al.*, 2004; Chen *et al.*, 2006). The ratios of OC/EC in the four seasons in Beibei were 7.0 ± 8.5, 7.4 ± 4.5, 3.1 ± 2.3, 7.9 ± 7.2 respectively, which were all larger than 2.0. The high ratios of OC/EC suggested that the measured OC was not only come from the direct emissions of particles as primary pollutants but also in the form of SOC formed by chemical reactions or produced by residential biomass burning and coal combustion (Shen *et al.*, 2017). In addition, it could be a heavy-duty diesel truck exhaust if the ratio of OC/EC was 0.8 (Hildemann *et al.*, 1991). Thus the value over 0.8 of the OC/EC ratios in all the four seasons (Table 2) would indicate a less heavy-duty diesel truck exhaust in the Beibei suburb, which was consistent with no direct industrial pollution sources within a 5-km distance of the sampling site in this study.

Turpin and Huntzicker (1991) found that the relationship between OC and EC could be further used to distinguish the source of carbon particles if OC had a good correlation with EC, which indicated that they came from the same source. Therefore, the correlation analysis of OC and EC could probably distinguish the source of carbon aerosol particles (Turpin *et al.*, 1990). From Fig. 4, a significant correlation between OC and EC in $PM_{2.1}$ in the Beibei suburb (R^2 = 0.43, P < 0.01) could indicate the same source for both OC and EC. Chen *et al.* (2006) reported that the air pollution could mainly derive from coal emissions when the ratio of OC/EC was between 2.5 and 10.5. As a result, the main air pollution source could be the coal

Table 4. Principal component analyses for seven carbonaceous aerosols in Beibei suburb of Chongqing Municipal City, Southwest China.

Composition	Factor1	Factor2	Factor3
OC_1	0.165	<u>0.466</u>	<u>0.861</u>
OC_2	0.485	<u>0.5</u>	–0.245
OC_3	<u>0.935</u>	0.189	–0.203
OC_4	<u>0.935</u>	0.169	–0.054
EC_1	<u>0.968</u>	0.077	–0.003
EC_2	0.769	–0.521	–0.048
EC_3	0.576	–0.572	0.447
Eigenvalue	3.869	1.136	1.047
Variance contribution rate (%)	55.3	16.2	15.0

The underlined values represent factor load values for the characteristic components of the recognition factors.
Abbreviations: EC_1, elemental carbon (580°C); EC_2, (740°C); EC_3, (840°C); and OC_1, organic carbon (140°C); OC_2, (280°C); OC_3, (480°C); OC_4, (580°C).

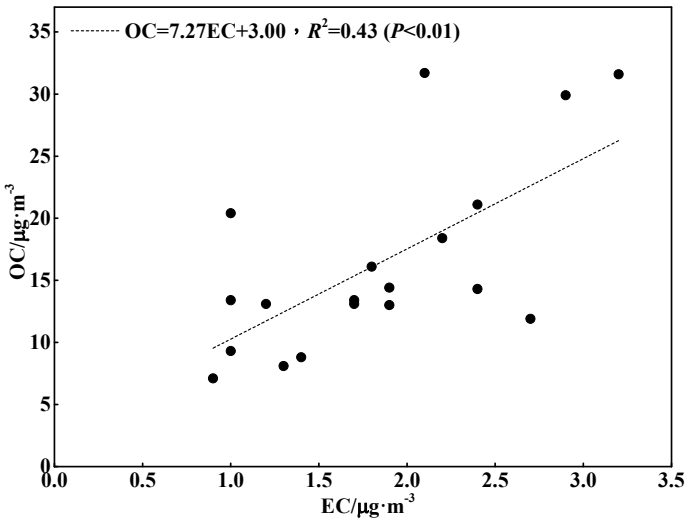

Fig. 4. Correlation analyses between organic carbon (OC) and elemental carbon (EC) in $PM_{2.1}$ in Beibei District, a suburb of Chongqing Municipal City, Southwest China.

emission as the slope of the correlation curve of OC and EC in $PM_{2.1}$ was 7.27 in the Beibei suburb.

One of the unique features of the IMPROVE protocol was that it can provide the concentrations of seven fractions for carbonaceous aerosol particles (Chow *et al.*, 1993, 2001). The abundances in each seven fractions of carbonaceous aerosols had been utilized to distinguish different emission sources of carbonaceous aerosols (Chow *et al.*, 2003, 2004a).

The concentrations of OC_1, OC_2, OC_3, OC_4, EC_1, EC_2 and EC_3 in $PM_{2.1}$ were 0.8 ± 0.5, 6.0 ± 2.9, 3.6 ± 1.6, 2.4 ± 1.3, 4.7 ± 3.7, 0.7 ± 0.3 and 0.1 ± 0.2 μg m^{-3}, accounting for 4.2%, 33.3%, 19.8%, 13.3%, 26.1%, 3.9% and 0.4% of the TC, respectively (Fig. 5). In general, OC_2, OC_3, OC_4 and EC_1 were the most abundant species in Beibei. Previous studies had showed that the abundance of OC_2, OC_3, OC_4, EC_1 and EC_2 might be associated with motor vehicle exhaust, EC_1 was the characteristic component of gasoline vehicle exhaust emissions, while EC_2 and EC_3 were enriched in diesel vehicle emission profile (Watson *et al.*, 1994; Chow *et al.*, 2004; Cao *et al.*, 2005). The concentrations of OC_2, OC_3, OC_4 and EC_1 in $PM_{2.1}$ were higher than the others, and the concentrations of EC_2 and EC_3 were the lowest (Fig. 5), indicating that the main pollution of carbonaceous aerosols in Beibei was the motor vehicle exhaust, especially gasoline vehicle emission. Cao *et al.* (2005) found that OC_2 accounted for 46.9% of TC in coal combustion samples, 29.2% in biomass burning samples and 30.5% in motor vehicle samples, and OC_1 was the characteristic emission component of biomass combustion (contributed 36.8% to TC in biomass burning samples). While the concentration of OC_1 in spring was higher than that in other three seasons (Fig. 5), and the annual average concentration of OC_2 was highest among the seven carbon components, indicating that more biomass was burned in spring, and the coal combustion was one of the main pollution sources of carbonaceous aerosols in Beibei. Chow *et al.* (2004a) also found that OC_3 (accounted 43% for OC) and EC_1 (accounted 93% for EC) were enriched in the cooking profile, while the concentrations of OC_3 and EC_1 were higher in spring and winter than those in summer and autumn (Fig. 5). This reflected that cooking was another pollution source of carbonaceous aerosols in Beibei, and more cooking emission in winter and spring might be related to more hot pot (a traditional typical gourmet food in Chongqing) was eaten in winter and spring.

To distinguish the different emission sources of carbonaceous aerosols in Beibei, PCA (principal component analysis) was used to analyze the seven fractions of carbonaceous aerosol in $PM_{2.1}$ samples by the SPSS software. The factors whose eigenvalue greater than 1 were extracted, and the factor value of different components was differentiated to make it easy to factor analysis by the method of orthogonal rotation. Then, the factor values used to identify the factor characteristic components were underlined, three factors with eigenvalues greater than 1 were finally obtained (Table 4).

Firstly, the contribution rate of Factor 1 was the highest in three factors and accounted for 55.3% of all seven fractions, with OC_3, OC_4 and EC_1 as the main contributors, while OC_3, OC_4, EC_1 and EC_2 were associated with motor vehicle emission, and EC_1 was the characteristic component of gasoline vehicle exhaust, so the Factor 1 might be connected with the gasoline vehicle exhaust. Secondly, the contribution of Factor 2 accounted for 16.2% of all seven fractions, with OC_1 and OC_2 as the main contributors, while Cao *et al.* (2005) found that OC_2 accounted for 46.9% of TC in coal combustion samples and OC_1 was the characteristic emission component of biomass combustion (contributed 36.8% to TC in biomass-burning samples), so the Factor 2 might be consisted with coal emission. Thirdly, the contribution of Factor 3 accounted for 15.0% of all seven fractions, which was close to Factor 2, was mainly affected by OC_1, which might be connected with biomass combustion. Thus the main pollution sources of carbonaceous aerosols in Beibei were gasoline vehicle exhaust, coal emission and biomass combustion.

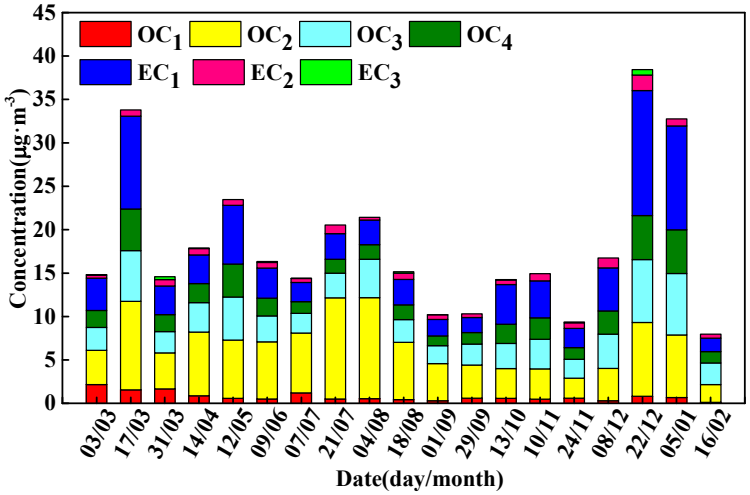

Fig. 5. Concentrations of seven carbonaceous aerosols over the whole year of 2014 in Beibei District, a suburb of Chongqing Municipal City, Southwest China. Abbreviations: EC_1, elemental carbon, 580°C; EC_2, 740°C; EC_3, 840°C; and OC_1, organic carbon, 140°C; OC_2, 280°C; OC_3, 480°C; OC_4, 580°C.

CONCLUSION

The carbonaceous aerosol was investigated on the campus of Southwest University in Beibei District, a suburb of Chongqing, China. During the period of sampling, the average annual concentrations of the OC and EC in the $PM_{2.1}$ and $PM_{9.0}$ were 16.3 ± 7.6 and 1.8 ± 0.7 μg m^{-3}, and 25.0 ± 9.6 and 3.2 ± 1.2 μg m^{-3}, respectively. The distribution of OC concentrations in the $PM_{2.1}$ was highly seasonal (winter > spring > summer > autumn), and increased biomass burning, for the purpose of preserving meat via smoking, may have accounted for the highest concentrations occurring in winter, whereas increased rainfall may have accounted for the lowest concentrations occurring in autumn. Meanwhile, the concentrations of OC in the $PM_{9.0}$ in winter were close to those in spring and summer but higher than those in autumn. By contrast, the $PM_{2.1}$ exhibited a more seasonal distribution of EC concentrations (winter > spring > summer > autumn), with the highest and lowest concentrations, occurring in winter and autumn, respectively, being attributable to the same factors that affected the OC. For $PM_{2.1}$, significantly positive and negative correlations existed between the OC and the wind speed and between the EC and the air temperature; however, for $PM_{9.0}$, significantly positive or negative correlations existed between the OC and the wind speed ($P < 0.01$) and between the OC and the relative humidity ($P < 0.05$), but no significant correlation was detected between the EC and any of the five meteorological factors. In addition, the OC and the EC were mainly concentrated in the fine particles (< 2.1 μm), and the former showed a bi-modal size distribution in all four seasons. Fine particles in the size range of 0.43–0.65 μm may have originated in vehicle exhaust and biomass combustion, whereas coarse particles in the size range of 4.7–5.8 μm may have originated in dust, suspended soil matter, and biological aerosols, such as microorganisms, plant fragments, and pollen. The EC in all four seasons only exhibited a peak in the coarse mode, in the size range of 4.7–5.8 μm, which may have been caused by direct combustion emissions of EC mixing with surface dust generated by tire/brake wear, road dust, industrial emissions, and particles from construction. Furthermore, the OC and the EC were significantly correlated ($P < 0.01$), and the average annual concentration of the SOC was 6.3 ± 5.9 μg m^{-3}, accounting for 33.5 ± 22.6% of the OC. Finally, analyses of the sources of atmospheric aerosol indicated that the pollution in Beibei was mainly derived from the exhaust of gasoline vehicles, biomass combustion, and coal combustion.

ACKNOWLEDGEMENTS

This study was jointly supported by the Key Program of National Natural Science Foundation of China (41230642), the National Natural Science Foundation of China (41275160), the Strategic Pilot Science and Technology Project of the Chinese Academy of Sciences (XDA05100100) and the Fundamental Research Funds for the Central Universities (XDJK2015A013).

REFERENCES

Ali, K., Panicker, A.S., Beig, G., Srinivas, R. and Acharja, P. (2016). Carbonaceous aerosols over Pune and Hyderabad (India) and influence of meteorological factors. *J. Atmos. Chem.* 73: 1–27.

Bi, X.H., Sheng, G.Y., Peng, P., Chen, Y.J. and Fu, J.M. (2005). Size distribution of *n*-alkanes and polycyclic aromatic hydrocarbons (PAHs) in urban and rural atmospheres of Guangzhou, China. *Atmos. Environ.* 39: 477–487.

Cao, J.J., Lee, S.C., Ho, K.F., Zhang, X.Y., Zou, S.C., Fung, K., Chow, J.C. and Watson, J.G. (2003). Characteristics of carbonaceous aerosol in Pearl River Delta Region, China during 2001 winter period. *Atmos. Environ.* 37: 1451–1460.

Cao, J.J., Wu, F., Chow, J.C., Lee, S.C., Li, Y., Chen, S.W., An, Z.S., Fung, K.K., Watson, J.G., Zhu, C.S. and Liu, S.X. (2005). Characterization and source apportionment of atmospheric organic and elemental carbon during fall and winter of 2003 in Xi'an, China. *Atmos. Chem. Phys.* 5: 3127–3137.

Cao, J.J., Hang, H., Lee, S.C., Chow, J.C., Zou, C.W., Ho, K.F. and Watson, J.G. (2012). Indoor/Outdoor relationships for organic and elemental carbon in $PM_{2.5}$ at residential homes in Guangzhou, China. *Aerosol Air Qual. Res.* 12: 902–910.

Chen, F., Zhang, X.H., Zhu, X.S., Zhang, H., Gao, J.X. and Hopke, P.K. (2017a). Chemical characteristics of $PM_{2.5}$ during a 2016 winter haze episode in Shijiazhuang, China. *Aerosol Air Qual. Res*. 17: 368–380.

Chen, Y., Xie, S.D., Luo, B. and Zhai, C.Z. (2014). Characteristics and origins of carbonaceous aerosol in the Sichuan Basin, China. *Atmos. Environ.* 94: 215–223.

Chen, Y., Wenger, J.C., Yang, F.M., Cao, J.J., Huang, R.J., Shi, G.M., Zhang, S.M., Tian, M. and Wang, H.B. (2017b). Source characterization of urban particles from meat smoking activities in Chongqing, China using single particle aerosol mass spectrometry. *Environ. Pollut.* 228: 92–101.

Chen, Y.J., Zhi, G.R., Feng, Y.L., Fu, J.M., Feng, J.L., Sheng, G.Y. and Simoneit, B.R.T. (2006). Measurements of emission factors for primary carbonaceous particles from residential raw-coal combustion in China. *Geophys. Res. Lett*. 33: 382–385.

Chow, J.C., Watson, J.G., Pritchett, L.C., Pierson, W.R., Frazier, C.A. and Purcell, R.G. (1993). The dri thermal/optical reflectance carbon analysis system: Description, evaluation and applications in U.S. Air quality studies. *Atmos. Environ.* 27: 1185–1201.

Chow, J.C., Watson, J.G., Lu, Z.Q., Lowenthal, D.H., Frazier, C.A., Solomon, P.A., Thuillier, R.H. and Magliano, K. (1996). Descriptive analysis of $PM_{2.5}$ and PM_{10} at regionally representative locations during SJVAQS/AUSPEX. *Atmos. Environ*. 30: 2079–2112.

Chow, J.C., Watson, J.G., Crow, D., Lowenthal, D.H. and Merrifield, T. (2001). Comparison of IMPROVE and NIOSH carbon measurements. *Aerosol Sci. Technol.* 34: 23–34.

Chow, J.C., Watson, J.G., Ashbaugh, L.L. and Magliano, K.L. (2003). Similarities and differences in PM_{10} chemical source profiles for geological dust from the San Joaquin Valley, California. *Atmos. Environ.* 37: 1317–1340.

Chow, J.C., Watson, J.G., Kuhns, H., Etyemezian, V., Lowenthal, D.H., Crow, D., Kohl, S.D. Engelbrecht, J.P. and Green, M.C. (2004a). Source profiles for industrial, mobile, and area sources in the Big Bend Regional Aerosol Visibility and Observational study. *Chemosphere* 54: 185–208.

Chow, J.C., Watson, J.G., Chen, L.W.A., Arnott, W.P., Moosmuller, H. and Fung, K. (2004b). Equivalence of elemental carbon by thermal/optical reflectance and transmittance with different temperature protocols. *Environ. Sci. Technol.* 38: 4414–4422.

Deng, X.J., Tie, X.X., Wu, D., Zhou, X.J., Bi, X.Y., Tan, H.B., Li, F. and Jiang, C.L. (2008). Long-term trend of visibility and its characterizations in the Pearl River Delta (PRD) region, China. *Atmos. Environ*. 42: 1424–1435.

Glaser, B., Dreyer, A., Bock, M., Fiedler, S., Mehring, M. and Heitmann, T. (2005). Source apportionment of organic pollutants of a highway-traffic-influenced urban area in Bayreuth (Germany) using biomarker and stable carbon isotope signatures. *Environ. Sci. Technol.* 39: 3911–3917.

Griffin, R.J., Dabdub, D. Kleeman, M.J., Fraser, M.P., Cass, G.R. and Seinfeld, J.H. (2002). Secondary organic aerosol 3. Urban/regional scale model of size and composition resolved aerosols. *J. Geophys. Res.* 107: AAC 5-1–AAC 5-14.

Gu, J.X., Bai, Z.P., Liu, A.X., Wu, L.P., Xie, Y.Y., Li, W.F., Dong, H.Y. and Zhang, X. (2010). Characterization of atmospheric organic carbon and element carbon of $PM_{2.5}$ and PM_{10} at Tianjin, China. *Aerosol Air Qual. Res.* 10: 167–176.

He, L.Y., Hu, M., Huang, X.F., Yu, B.D., Zhang, Y.H. and Liu, D.Q. (2004). Measurement of emissions of fine particulate organic matter from Chinese cooking. *Atmos. Environ*. 38: 6557–6564.

Hildemann, L.M., Markowski, G.R. and Cass, G.R. (1991). Chemical composition of emissions from urban sources of fine organic aerosol. *Environ. Sci. Technol*. 25: 744–759.

Huang, R.J., Zhang, Y.L., Bozzetti, C., Ho, K.F., Cao, J.J., Han, Y.M., Daellenbach, K.R., Slowik, J.G., Platt, S.M., Canonaco, F., Zotter, P., Wolf, R., Pieber, S.M., Bruns, E.A., Crippa, M., Ciarelli, G., Piazzalunga, A., Schwikowski, M., Abbaszade, G., Schnelle-Kreis, J., Zimmermann, R., An, Z.S., Szidat, S., Baltensperger, U., Haddad, I.E. and Prevot, A.S.H. (2014). High secondary aerosol contribution to particulate pollution during haze events in China. *Nature* 514: 218–222.

Jacobson, M.Z. (2001). Strong radiative heating due to the mixing state of black carbon in atmospheric aerosols. *Nature* 409: 695–697.

John, W., Wall, S.M., Ondo, J.L. and Winklmayr, W. (1990). Modes in the size distributions of atmospheric inorganic aerosol. *Atmos. Environ.* 24: 2349–2359.

Kirkevag, A., Iversen, T., Seland, O., Hoose, C., Kristjansson, J.E., Struthers, H., Ekman, A.M.L., Ghan, S., Griesfeller, J., Nilsson, E.D. and Schulz, M. (2013). Aerosol-climate interactions in the Norwegian Earth System Model-NorESM1-M. *Geosci. Model Dev.* 6: 207–244.

Kumar, P. and Yadav, S. (2016). Seasonal variations in water soluble inorganic ions, OC and EC in PM_{10} and $PM_{>10}$ aerosols over Delhi: Influence of sources and meteorological factors. *Aerosol Air Qual. Res.* 16: 1165–1178.

Lan, Z.J., Chen, D.L., Li, X.A., Huang, X.F., He, L.Y. and Deng, Y.G. (2011). Modal characteristics of carbonaceous aerosol size distribution in an urban atmosphere of South China. *Atmos. Res.* 100: 51–60.

Lang, J.L., Zhang, Y.Y., Zhou, Y., Cheng, S.Y., Chen, D.S., Guo, X.U., Chen, S., Li, X.X., Xing, X.F. and Wang,

H.Y. (2017). Trends of $PM_{2.5}$ and chemical composition in Beijing, 2000-2015. *Aerosol Air Qual. Res.* 17: 412–425.

Li, T.C., Yuan, C.S., Lo, K.C. Hung, C.H., Wu, S.P. and Tong, C. (2015). Seasonal variation and chemical characteristics of atmospheric particles at three islands in the Taiwan Strait. *Aerosol Air Qual. Res.* 15: 2277–2290.

Lim, Y.B., Tan, Y., Perri. M.J., Seitzinger, S.P. and Turpin, B.J. (2010). Aqueous chemistry and its role in secondary organic aerosol (SOA) formation. *Atmos. Chem. Phys.* 10: 10521–10539.

Liu, X.F., Peng, L., Bai, H.L. and Mu. L. (2015). Characteristics of organic carbon and elemental carbon in the ambient air of coking plant. *Aerosol Air Qual. Res.* 15: 1485–1493.

Mauderly, J.L. and Chow, J.C. (2008). Health effects of organic aerosols. *Inhalation Toxicol.* 20: 257–288.

Mcmurry, P.H. and Zhang, X.Q. (1989). Size distributions of ambient organic and elemental carbon. *Aerosol Sci. Technol.* 10: 430–437.

Niu, Z.C., Zhang, F.W., Kong, X.R., Chen, J.S., Yin, L.Q. and Xu, L.L. (2012). One-year measurement of organic and elemental carbon in size-segregated atmospheric aerosol at a coastal and suburban site in Southeast China. *J. Environ. Monit.* 14: 2961–2967.

Odum, J.R., Hoffmann, T., Bowman, F., Collins, D., Flagan, R.C. and Seinfeld, J.H. (1996). Gas/particle partitioning and secondary organic aerosol yields. *Environ. Sci. Technol.* 30: 2580–2585

Pandis, S.N., Harley, R.A., Cass, G.R. and Seinfeld, J.H. (1992). Secondary organic aerosol formation and transport. *Atmos. Environ.* 26: 2269–2282.

Pavuluri, C.M., Kawamura, K., Uchida, M., Kondo, M. and Fu, P.Q. (2013). Enhanced modern carbon and biogenic organic tracers in Northeast Asian aerosols during spring/summer. *J. Geophys. Res.* 118: 2362–2371.

Pope, C.A. and Dockery D.W. (2006). Health effects of fine particulate air pollution: Lines that connect. *J. Air Waste Manage. Assoc.* 56: 709–742.

Salma, I., Maenhaut, W. and Zaray, G. (2002). Comparative study of elemental mass size distributions in urban atmospheric aerosol. *J. Aerosol Sci.* 33: 339–356.

Schauer, J.J., Kleeman, M.J., Cass, G.R. and Simoneit, B.R.T. (1999a). Measurement of emissions from air pollution sources. 1. C_1-C_{29} organic compounds from meat charbroiling. *Environ. Sci. Technol*. 33: 1566–1577.

Schauer, J.J., Kleeman, M.J., Cass, G.R. and Simoneit, B.R.T. (1999b). Measurement of emissions from air pollution sources. 2. C_1-C_{30} organic compounds from medium duty diesel trucks. *Environ. Sci. Technol*. 33: 1578–1587.

Schauer, J.J., Kleeman, M.J., Cass, G.R. and Simoneit, B.R.T. (2001). Measurement of emissions from air pollution sources. 3. C_1-C_{29} organic compounds from fireplace combustion of wood. *Environ. Sci. Technol*. 35: 1716–1728.

Schauer, J.J., Kleeman, M.J., Cass, G.R. and Simoneit, B.R.T. (2002a). Measurement of emissions from air pollution sources. 4. C_1-C_{27} organic compounds from cooking with seed oils. *Environ. Sci. Technol*. 36: 567–575.

Schauer, J.J., Kleeman, M.J., Cass, G.R. and Simoneit, B.R.T. (2002b). Measurement of emissions from air pollution sources. 5. C_1-C_{32} organic compounds from gasoline-powered motor vehicles. *Environ. Sci. Technol*. 36: 1169–1180.

Shen, Z.X., Zhang, Q., Cao, J.J., Zhang, L.M., Lei, Y.L., Huang, Y., Huang, R.J., Gao, J.J., Zhao, Z.Z., Zhu, C.S., Yin, X.L., Zheng, C.L., Xu, H.M. and Liu, S.X. (2017). Optical properties and possible sources of brown carbon in $PM_{2.5}$ over Xi'an, China. *Atmos. Environ*. 150: 322–330.

Turpin, B.J., Cary, R.A. and Huntzicker, J.J. (1990). An in situ, time-resolved analyzer for aerosol organic and elemental carbon. *Aerosol Sci. Technol.* 12: 161–171.

Turpin, B.J. and Huntzicker, J.J. (1991). Secondary formation of organic aerosol in the Los-Angeles Basin: A descriptive analysis of organic and elemental carbon concentrations. *Atmos. Environ.* 25: 207–215.

Turpin, B.J. and Huntzicker, J.J. (1995). Identification of secondary organic aerosol episodes and quantification of primary and secondary organic aerosol concentrations during SCAQS. *Atmos. Environ*. 29: 3527–3544.

Whitby, K.T., Husar, R.B. and Liu, B.Y.H. (1972). The aerosol size distribution of Los Angeles smog. *J. Colloid Interface Sci.* 39: 177–204.

Yang, H., Li, Q.F. and Yu, J.Z. (2003). Comparison of two methods for the determination of water-soluble organic carbon in atmospheric particles. *Atmos. Environ*. 37: 865–870.

Ye, D., Zhao, Q., Jiang, C.T., Chen, J. and Meng, X.X. (2007). Characteristics of elemental carbon and organic carbon in PM_{10} during spring and autumn in Chongqing, China. *China Part.* 5: 255–260.

Yu, H., Wu, C., Wu, D. and Yu, J.Z. (2009). Size distributions of elemental carbon and its contribution to light extinction in urban and rural locations in the Pearl River Delta Region, China. *Atmos. Chem. Phys*. 10: 5107–5119.

Zhang, L.Y., Huang, Y.M., Liu, Y., Yang, F.M., Lan, G.X., Fu, C. and Wang, C. (2015). Characteristics of carbonaceous species in $PM_{2.5}$ in Wanzhou in the hinterland of the Three Gorges Reservoir of Northeast Chongqing, China. *Atmosphere* 6: 534–546.

Zheng, B., Zhang, Q., Zhang, Y., He, K.B., Wang, K., Zheng, G.J., Duan, F.K., Ma, Y.L. and Kimoto, T. (2015). Heterogeneous chemistry: A mechanism missing in current models to explain secondary inorganic aerosol formation during the January 2013 haze episode in North China. *Atmos. Chem. Phys.* 15: 2031–2049.

Received for review, November 30, 2017
Revised, June 26, 2018
Accepted, August 28, 2018